Characterisation and activity of mixed metal oxide catalysts for the gas-phase selective oxidation of toluene

Maria-Luisa Palacios, Stan Golunski, Graham J Hutchings* and Stuart H. Taylor*

Cardiff Catalysis Institute, School of Chemistry, Cardiff University, Main Building, Park Place, Cardiff, CF10 3AT, UK.

Corresponding authors: taylorsh@cardiff.ac.uk; +44 (0)29 2087 4062

hutch@cardiff.ac.uk; +44 (0)29 2087 4059

Abstract

Mixed metal bi-component oxide catalysts, including Fe/Mo, U/Mo, U/W, Fe/U, U/V and U/Sb have been prepared, characterised and evaluated for gas phase selective toluene oxidation. Selective toluene oxidation activity to form benzaldehyde was exhibited by Fe/Mo, U/Mo and U/W mixed oxide catalysts. The Fe/Mo catalyst produced the highest benzaldehyde yield. Catalysts that formed benzaldehyde also produced a range of by-products, these were other partial oxidation and coupling products, and preliminary studies of benzaldehyde oxidation suggests they were formed from secondary reactions of benzaldehyde. The Fe/U, Sb/U and U/V catalysts produced only total oxidation to carbon oxides. Catalysts were characterised by X-ray diffraction, laser Raman spectroscopy and temperature programmed reduction. Single molybdate phases were identified for the Fe/Mo and U/Mo catalysts, and a mixture of uranium molybdate and WO_3 was identified for the U/W catalyst. Results suggest that the formation of a molybdate phase is important for the selective oxidation of toluene. In contrast, the U/Fe

catalyst was a mixture of U_3O_8 and V_2O_5, whilst the Fe/U catalyst was comprised of highly dispersed iron oxide on UO_3. The presence of U_3O_8 was responsible for toluene total oxidation. The U/Sb catalyst did not exhibit selective toluene oxidation, but previous studies have demonstrated that the catalyst exhibits high activity for selective propene oxidation. Similar behaviour has been observed for the other catalysts in this study, and it is apparent that catalysts that were selective for toluene oxidation were not selective for propene/propane oxidation and vice versa.

Keywords: catalytic selective oxidation, mixed oxides, toluene, benzaldehyde, uranium, molybdenum, tungsten

1. Introduction

Selective oxidation to partially oxidised products is an important research aim; and provides a facile route for the functionalisation of hydrocarbons. Within the field of heterogeneous catalytic oxidation much research effort has focussed on hydrocarbon partial oxidation to commercially more valuable products. Achieving high selectivity in hydrocarbon oxidation is especially challenging, as thermodynamically oxidation favours the formation of carbon dioxide and water. The oxidation of aromatic compounds is potentially a facile process for the production of oxygenated derivatives. Toluene can be converted to benzaldehyde, benzoic acid and benzyl benzoate, as well as a range of other products, and these are commercially significant as versatile intermediates in the manufacture of pharmaceuticals, dyes, solvents, perfumes, plasticizers, dyestuffs, preservatives and flame retardants. Currently benzaldehyde is produced commercially by the chlorination of toluene followed by saponification [1], which is a more complex process than direct partial oxidation. Relatively recently efficient toluene

selective oxidation by oxygen in the liquid phase has been achieved in a batch process using titania supported gold-palladium nanoparticles [2]. However, interest still remains for selective toluene oxidation in a gas phase flow process.

The gas-phase selective oxidation of toluene has been studied using heterogeneous catalysts based on various single and mixed metal oxides, with the majority of studies using molybdenum and vanadium oxide systems [3,4,5,6]. The aim of this study is to synthesise, characterise and explore more fully the use of mixed metal oxide systems, especially those containing uranium, as it has a well-established history as a selective oxidation catalyst component. These include Fe/Mo, U/Mo, Fe/U, Sb/U and V/U oxide catalysts, as mixed metal oxides with these elements have been prepared previously. The catalysts selected for this study have been chosen for several reasons; in particular uranium oxide is a central component of some selective oxidation catalysts, and it is a component that is not often currently studied. The actinide elements exhibit an electronic structure with 86 electrons, surrounded by valence electrons in the 7*s*, 6*d* and 5*f* shells. Uranium oxides are generally presented as ionic solids. However, an alternative interpretation involves covalent bonding with the formation of new molecular orbitals from effective overlapping of appropriate atomic orbitals of similar energy. These two descriptions are limiting cases, and actinide compounds are often best described as partially ionic and partially covalent. The electronic structures of these elements and their compounds are determined by a strong competition between the 5*f*, 6*d* and 7*s* electrons. In uranium these shells are so close in energy that hybridisation of the 5*f* and 6*d* electrons can occur. Hence the unique electronic properties of uranium give the element the potential for many interesting catalytic properties [7].

Uranium has six valence electrons, and it is therefore similar in nature to the transition elements chromium, molybdenum and tungsten. It can also show structural similarities with MoO_3 and WO_3.In particular, molybdenum and tungsten are oxides forming the basis of catalysts for many

selective oxidation reactions, for example $Fe_2(MoO_4)_3$ is used as a commercial catalyst for the selective oxidation of methanol to formaldehyde [8]. Uranium oxides also exist in a variety of different forms, with some of the most common being UO_2, U_4O_9, U_3O_7, U_3O_8 and UO_3. These oxides exhibit a range of oxidation states, and in some cases mixed oxidation states. Furthermore, uranium oxides also have extensive redox properties with the ability to show a wide range of nonstoichiometry and semiconducting behaviour. Against this background uranium oxide is a flexible catalyst component, as it have versatile properties, many of which are important for catalytic selective oxidation reactions.

Pioneering work by Grasselli and co-workers developed mixed uranium-antimony oxide catalysts for the commercial selective oxidation and ammoxidation of propylene to acrolein and acrylonitrile [9,10,11]. The structure of USb_3O_{10} is critical for selective oxidation, and the phase is structurally complex. Uranium is present in a single environment, whilst antimony is in two and oxygen in four different environments. The structure comprises of layers, which contain heavy atoms and oxygen alternating with layers of oxygen only. Five layers of planes containing heavy metal atoms are required to completely describe the unit cell of USb_3O_{10}. There are two types of lattice oxygen in the structure, one giving high selectivity for partial oxidation, and the other, which was less active and selective, producing carbon oxides [11].

Optimum performance was only observed with the USb_3O_{10} phase, and catalyst preparation is crucial to achieve the correct phase as a number of other structures are possible. The $USbO_5$ structure is very similar to that of USb_3O_{10} and it is proposed as a precursor to USb_3O_{10}, which again decomposes at high temperature to $USbO_5$ [11,12]. The elegant work of Grasselli and co-workers has inspired many studies, and more recent work has investigated alternative methods, such as hydrothermal synthesis for the preparation of uranium-antimony mixed selective oxidation catalysts [13]. We have also used the work of Grasselli and co-workers as inspiration for investigating the current range of uranium-containing two-component mixed metal oxide

catalysts for selective oxidation, and this approach forms the basis of a large part of the present study.

2. Experimental

Catalyst preparation

The Fe/U (atomic ratio Fe/U = 0.5/3) was prepared using a co-precipitation method. $Fe(NO_3)_3.9H_2O$ (1 g, Aldrich 99.99+%) was dissolved in deionised water (10 ml) and added to a solution of $UO_2(NO_3).2H_2O$ (5.85 g, Strem 99+%), in deionised water (16 ml). The two solutions were mixed and the excess water evaporated overnight at 150 °C. The solid obtained was calcined (450 °C, 3 h) in static air to produce the catalyst.

The U/Sb catalyst was synthesised using methods described in the literature, reacting $UO_2(NO_3).2H_2O$ (8.8 g, Strem 99+%) with Sb_2O_3 (8.7 g, Aldrich 99.99%) dissolved in 70% nitric acid and refluxed for 3 h [9,11]. After cooling, the solution was adjusted to pH 8 by adding 28% aqueous NH_4OH solution. The solid product was filtered, washed with deionised water and dried (120 °C, 24 h) to produce the precursor of the catalyst. The precursor was then calcined (425 °C, 16 h) and the temperature increased to 925 °C for a further 16 h. The catalysts produced by this procedure had an excess of antinomy, observed by XRD, in the form of the oxide. The contaminating Sb_2O_3 was removed by refluxing the catalyst with aqueous HCl at 100 °C to produce the final catalyst.

The U/Mo catalysts were synthesised using a method described in the literature [4]. A solution was prepared by dissolving $U(CH_3COO)_2.2H_2O$ (5.4 g, BDH AnalaR grade) in deionised water (19.6 ml). The solution was added to a solution of $(NH_4)_6Mo_7O_{24}.4H_2O$, (0.4 g, Aldrich) dissolved in hot deionised water (20 ml). The excess water was evaporated and the resulting solid calcined in flowing air (550 ^oC, 4 h).

The Fe/Mo catalyst was prepared by a precipitation method [14]. $Fe(NO_3)_3.9H_2O$ (2.0 g, Aldrich 99.99+%) was dissolved in deionised water (15 ml) and added to a solution of $(NH_4)_6Mo_7O_{24}.4H_2O$ (1.3 g, Aldrich) dissolved in deionised water (10.5 ml). The resulting precipitate was dried and calcined in static air (400 °C, 6 h and then 750 °C, 24 h).

The U/W catalyst was prepared following a procedure previously described in the literature [15]. Preparation was via heating a physical mixture of U_3O_8 (10 g, Strem) and WO_3 (8.26 g, Aldrich) at 700 °C for 24 h and then at 800 °C for 72 h in static air. The U/V catalyst was also prepared by heating a physical mixture of V_2O_5 (1.82 g, Aldrich 99.99+%), V_2O_3 (0.3 g, Aldrich 99.99+%) and U_3O_8 (6.7 g, Strem) at 550 °C for 24 h in flowing nitrogen.

Catalyst characterisation

Powder X-ray diffraction (XRD) studies were performed using an Enraf Nonius FR590 instrument with a Cu source operated at an X-ray power of 1.2 kW (30 mA, 40 kV). A Ge(111) single crystal monochromator was used to select Cu $K\alpha_1$ X-rays for analysis. The powdered samples were compressed into an aluminium sample holder, which was rotated during data collection to compensate for any ordering of crystallite orientation, which may occur during sample preparation. The diffraction pattern was measured by means of a position sensitive detector (Inel PSD120), covering 2θ values over the range 4.4-124.6°. Raw data were corrected against a silicon standard, and phase identification was performed by matching the experimental pattern against standard entries in the ICDD database.

Catalyst surface areas were measured by the BET method, using a Micromeritics ASAP 2010 apparatus. Prior to determination catalysts were degassed at 75 °C for 6 h. Measurements were carried out at -196 °C using multiple point high purity nitrogen adsorption.

Laser Raman spectroscopy (LRS) analysis was performed using a Renishaw system 1000 laser Raman microscope. An argon ion laser (514.5 nm) was used as excitation source and was

typically operated at a power of 20 mW. All the samples were used in powdered form and were placed on a microscope slide and the laser focused on the sample to produce a spot size of *ca.* 3 μm in diameter. Spectra were collected using a back-scattering geometry with an 180° angle between the illuminating and the collected light. In certain studies the laser power was varied by using a series of filters. The laser was focused onto the sample by means of an Olympus BH2-UMA optical microscope.

The apparatus used for temperature programmed reduction (TPR) was a TPR/TPO/TPD Micromeritics Autochem 2900 equipped with a TCD detector. The reducing gas used in all experiments was 10%H_2 in Ar, with a flow rate of 50 ml min^{-1}. The temperature range explored was from room temperature to 1000 °C with a ramp rate of 10 °C min^{-1}. The sample mass was varied (25-100 mg) depending on the sample and details of specific conditions are given with the TPR profiles.

Catalyst activity

Catalytic activity was determined in a fixed bed plug flow microreactor. Helium and oxygen flow rates were controlled with electronic thermal mass flow controllers. The gases flowed into a vaporiser thermostatically controlled at 120 °C, and were mixed with toluene vapour, which was injected by a syringe pump. The reactor tube (i.d 13 mm) was held vertically and was constructed from Pyrex. The catalyst was held in the middle of the reactor tube, supported upon a porous sintered quartz frit. The catalyst bed was heated by a ceramic tube furnace and the temperature controlled by a thermocouple placed in intimate contact with the catalyst bed. The outlet of the reactor was heated to 170 °C with a heating tape in order to minimise condensation of reactants and products. At the end of an experiment the catalyst was cooled down in a flow of He with all lines heated. The total gas flow rate was 27.75 ml min^{-1} with the ratio of toluene/oxygen/helium = 1/16/83. The catalyst was loaded to a constant volume of 0.45 cm^3

for all experiments; resulting in a gas hourly space velocity (GHSV) of 3,700 h^{-1}. Product analysis was performed on-line using a Varian 3400 GC with thermal conductivity and flame ionisation detectors. Separation was achieved using Poropak Q (2 m x 1/8" o.d.) and Molecular sieve 13X (2 m x 1/8" o.d.), with the columns connected in a series/by-pass configuration. Using a suitable temperature programmed regime it was possible to separate and quantify the products and reactants with a single analysis. Toluene conversion was calculated from the difference between the concentrations in the reactor exit gas at a given temperature as a percentage of the toluene concentration in the reactant feed. Selectivities were defined as the percentage product formed in relation to the total products measured in the gas phase, after correction for the number of carbon atoms. Carbon balances were in the range of95-105 %.

3. Results

Catalyst characterisation

The atomic ratio of the catalyst as synthesised and the BET surface areas are presented in Table 1. The surface areas of the catalysts were diverse, and very low surface areas (<1 $m^2 g^{-1}$) were determined for the U/Mo, Fe/Mo and U/V catalysts. The surface area of the U/W catalyst was also very low, however, the surface areas of U/Sb and U/Fe were significantly greater, at 25 and 18 $m^2 g^{-1}$ respectively.

The phases identified from powder X-ray diffraction are summarised in Table 1. The presence of single mixed oxide phases, with no other contaminating crystalline phases, were confirmed for the Fe/Mo, U/Mo, and U/Sb catalysts. In the first two systems molybdate phases were identified, these were iron molybdate ($Fe_2(MoO_4)_3$) and uranyl molybdate (UO_2MoO_4) respectively. In the case of the U/Sb catalyst the USb_3O_{10} phase was observed and there was no evidence for excess Sb_2O_3 which was identified during preparation. On the contrary, the remaining catalysts were a mixture of single oxides or mixtures of single oxides and mixed oxides. The former has been confirmed for the U/V system as the phases identified were U_3O_8

and V_2O_5, and for the U/Fe system were only the UO_3 phase was observed. Whilst for the U/W catalyst a mixture of bulk WO_3 and UO_2WO_4 was identified.

The catalysts were investigated using laser Raman spectroscopy, and by virtue of analysis by back scattered light LRS is a more surface sensitive technique compared to the bulk analysis of powder XRD. The combination of both techniques provides an excellent set of tools for characterisation. In all cases the spectra were compared with the spectra of their respective single oxide components and appropriate reference compounds.

The Raman spectrum of the U/Mo oxide catalyst exhibited bands in the 955-165 cm^{-1} region (Figure 1). The most intense Raman bands were observed at 747 and 761 cm^{-1}, whilst significant bands were also observed at 955 and 886 cm^{-1}. A further series of peaks were centred around 330 cm^{-1}. Raman spectra of $(NH_4)_6Mo_7O_{24}.4H_2O$ and MoO_3 have also been recorded for referencing purposes.

The Raman spectra of the Fe/Mo mixed oxide catalyst is presented in Figure 2. The most intense Raman band was at 783 cm^{-1}, with further major bands at 821, 937, 967 and 991 cm^{-1}. Iron(III) oxide was also studied by Raman spectroscopy as a reference material. The U/Sb oxide catalyst is shown in Figure 3. The most intense Raman band was observed at 491 cm^{-1}. The remaining Raman bands were relatively broad, and with the exception of the peak at 205 cm^{-1}, they were also of relatively low intensity. The spectrum showed an increasing background indicative of sample fluorescence from the excitation source. Antimony oxides, Sb_2O_3 and Sb_2O_4, were also studied to aid spectral assignment.

The Raman spectrum of the Fe/U catalyst showed relatively few active bands and these were also relatively broad (Figure 4). The most intense band in the U/Fe spectrum was at 762 cm^{-1}, with much less intense broad features at 821 477 and 322 cm^{-1}.

The Raman spectrum of the U/V mixed oxide catalyst is shown in Figure 5. Raman studies demonstrated sample fluorescence, despite the fluorescence the Raman active bands are

extremely well-defined with the dominant band at 997 cm^{-1}. Strong Raman bands were also observed at 703, 528 and 286 cm^{-1}. For comparison V_2O_5 was used as a reference material.

The Raman spectrum of the U/W oxide catalyst showed a large number of Raman bands (Figure 6). Intense bands were observed at 806, 717 and 272 cm-1 and generally these were broader than the other lower intensity peaks in the spectrum.

Temperature programmed reduction studies were performed on the Mo/U, Fe/Mo, Fe/U and U/W catalysts. The TPR profile for the U/Mo mixed oxide catalyst showed three peaks at 614, 653 and 780 °C (Figure 7). In the case of the Fe/Mo mixed oxide catalyst the TPR profile was better resolved when a larger sample mass was used. In fact only the profile obtained with 70 mg of catalyst was resolved into four peaks at 670, 767, 831 and 951 °C (Figure 8). The TPR profile for the U/W mixed oxide catalyst is shown in Figure 9. Three peaks were observed at 738, 843 and 891 °C. For the Fe/U mixed oxide the TPR profile revealed important information, regarding the structure of the catalyst (Figure 10). The profile exhibited two reduction maxima at 489 and 576 °C.

Catalytic activity

Activity studies were carried out in the temperature range from 150 °C to 530 °C, although data summarised in Table 8, are generally from 300 °C, as no significant activity was observed below this temperature. Carbon balances for detected gas phase products were generally 100 ±5%, although for some experiments when higher yields of benzaldehyde were observed this value decreased significantly. Blank experiments in an empty reactor showed only trace activity at 500 °C, suggesting that reactions of toluene in the gas phase and those initiated by the reactor walls were negligible over the temperature range investigated.

The mixed oxide catalysts Mo/U, Fe/Mo and U/W were all active for toluene selective oxidation to benzaldehyde in varying degrees. The other gaseous products from these catalysts were

carbon oxides, with trace quantities of aromatic oxidative coupling products, which were analysed off-line by NMR spectroscopy and GC-MS. The best catalytic results for toluene selective oxidation were obtained using the Fe/Mo oxide, which produced a conversion of 43% and selectivity to benzaldehyde of 86% at 400 °C. The U/Mo catalyst also demonstrated appreciable conversion and selectivity to benzaldehyde, and at 500 °C a 90% conversion of toluene and 13% selectivity towards benzaldehyde was observed. Selective toluene oxidation was also evident over the U/W catalyst, which produced benzaldehyde at 475 °C with 5% selectivity; the toluene conversion under these conditions was 74%. The yields of benzaldehyde produced by the Fe/Mo, U/Mo and U/W oxide catalysts, albeit relatively low, are comparable with the per pass yields from other studies [4]. The per pass yield of benzaldehyde obtained from the Fe/Mo catalyst at 400 °C was particularly noteworthy.

In addition to gaseous products, the Fe/Mo, U/Mo and U/W mixed oxide catalysts also formed solid products, and these were characterised by NMR spectroscopy. There was a significant quantity of solid products produced from the Fe/Mo catalyst and benzaldehyde, benzoyl peroxide and benzoic acid were identified. At 450 °C and above the Fe/Mo catalyst showed deactivation, and this was due to deposition of solid reaction products throughout the catalyst bed and the reactor, evidenced by a decrease in the carbon balance measured from the gaseous products detected. A similar array of solid products was also detected for the U/Mo and U/W catalysts, although they were not as active for benzaldehyde production, and formed less deposited solid products, and did not demonstrate the same deactivation as the more active Fe/Mo catalyst.

The U/Sb, U/V and Fe/U catalysts were active for toluene oxidation, however, they were not selective for partial oxidation as none produced benzaldehyde. The only gaseous products detected from these catalysts were those of deep oxidation. The Fe/U and U/V catalysts were the most active in this study, both exhibited appreciable conversion at 300 °C. The catalysts

based on U/Sb and U/V only produced CO_2, whilst the U/Sb system was considerably less active than U/V and only showed 28% toluene conversion at 530 °C. The U/V catalyst also produced CO in addition to CO_2, although CO_2 selectivity was always >96%. It was also evident that the U/Sb, U/V and Fe/U mixed oxide catalysts did not produce any of the aromatic coupling products or solid products which were produced from the catalysts which were active for toluene partial oxidation to benzaldehyde.

4. Discussion

Catalyst structure

The structure of the U/Mo oxide catalyst can be determined from comparison of the Raman vibrational data with a series of reference molybdenum and uranium compounds, these include $(NH_4)_6Mo_7O_{24}.4H_2O$, MoO_3, uranyl nitrate and various oxides (Table 2). There are two common coordination states for molybdates, these are tetrahedral (Td) in the MoO_4^{2-} unit and octahedral (Oh) in the $Mo_7O_{24}^{6-}$ unit [16].

$$7MoO_4^{2-} + 8H^+ \Leftrightarrow Mo_7O_{24}^{6-} + 4H_2O$$

The position of the Mo=O symmetric stretching vibrational band of MoO_4^{2-} is at 955 cm^{-1}, and therefore confirms the presence of the tetrahedral structure [17]. The band at 886 cm^{-1} is probably due to the asymmetric stretching vibration of the Mo=O of the MoO_4^{2-} tetrahedral molybdate and corresponds well with tetrahedrally coordinated crystalline K_2MoO_4 []. Some uncertainty on the assignation of this band still remains due to the fact that the band at 886 cm^{-1} could also be due to the symmetric stretching vibration of the uranyl ion [14]. Bands at 799, 793, and 747 cm^{-1} are due to asymmetric stretching vibrations in Mo-O-Mo bonds. The band at 761 cm^{-1} is proposed to be the symmetric stretching O-U-O-U vibration, although the frequency

is shifted from that expected for the common oxides of uranium, confirming that discrete uranium oxide phases were not present [17]. The Mo-O-Mo bending vibration bands are at 368 cm^{-1} and 224 cm^{-1}, whilst the bending vibration of O-U-O is present at 347 cm^{-1}.

The Raman assignment of the Fe/Mo mixed oxide catalyst is shown in Table 3. The main Raman band of the Fe/Mo catalyst was at 783 cm^{-1} and corresponds to the asymmetric stretching vibration Mo-O-Mo of the MoO_4^{2-} tetrahedral molybdate. The weak Raman features due to the symmetric stretching vibrations of Mo=O of the MoO_4^{2-} tetrahedral molybdate were observed at 967 and 937 cm^{-1}. The band at 821 cm^{-1} was attributed to asymmetric stretching vibration Mo=O of the MoO_4^{2-}. The band at 991 cm^{-1} is best assigned to an Mo=O vibration of an MoO_3 phase, however, no evidence for a MoO3 phase was apparent from the XRD data. It is also possible that the band could be due to the Mo=O vibration of the molybdate phase which is shifted by the incorporation of iron. The absence of MoO_3 signatory bands at 917 and 665 cm^{-1} support the suggestion that MoO3 is not present in addition to the molybdate phase.

The detailed assignment of the Raman active bands in the U/Sb mixed oxide catalyst is more difficult as there is little previous Raman data on the mixed oxide, which has a large and complex unit cell [18]. The structure of the mixed oxide has a variety of different coordinations for both uranium and antimony. General assignments have been made and these are shown in Table 4. Bands in the region *ca.* 304 cm^{-1} are in the bending region and are attributed to U-O-U and Sb-O-Sb. The other two groups of bands at 345-560 cm^{-1} and 776-905 cm^{-1} are assigned to symmetric and asymmetric stretching vibrations of U-O and Sb-O. The most significant observation from the Raman data is that the active bands in the mixed oxide spectrum do not correspond to those in the spectra of the antimony and uranium single oxides. In the case of the Fe/Mo, U/Mo and U/Sb catalysts the formation of mixed oxide phases were confirmed, and this was in good agreement with the results obtained by XRD.

Raman data are summarised for the Fe/U catalyst in Table 5. The main band in the spectra at 762 cm^{-1} was due to U-O stretching vibration, which along with the weaker band at 822 cm^{-1} is characteristic of the simple Raman spectra of UO_3 (Table 3). Both bands are slightly shifted to lower wave number when compared to UO_3, and this is probably due to a chemical interaction between iron and uranium components. There is no strong evidence for the presence of a discrete iron oxide phase, although the low frequency Raman feature at 322 cm^{-1} is centred in the region of the most intense features in the spectra of Fe_2O_3, and bands from UO3 are not generally observed in this region [17]. The presence of iron oxide is a tentative suggestion based on the Raman studies, and the absence of any X-ray diffracting domains indicated that the iron oxide is either amorphous or it has a small crystallite size.

Table 6 shows the comparison between the Raman spectra of the U/V oxide catalysts and V_2O_5 reference material. Both Raman spectra were similar and the positions of the bands were within 1-2 wavenumbers of each other. Bulk U_3O_8 was also identified by XRD, however, this phase was not identified from the Raman analysis. U_3O_8 has an intense dark green/black colour and Raman spectroscopy is notoriously difficult due to black body effects. The most intense Raman bands from U_3O_8 are at 738 and 811 cm^{-1} and are weak compared to those from V_2O_5. The similarity of the Raman data between the U/V oxide catalysts and V_2O_5 indicates that there is little interaction between the separate uranium and vanadium oxide phases.

The U/W oxide catalysts showed features corresponding to a WO_3 phase, these were clearly visible at 806, 717 and 272 cm^{-1} (Table 7), and are consistent with XRD data. Powder XRD also indicated that the catalyst contained a crystalline uranyl tungstate phase (UO_2WO_4), and the Raman bands at 953 and 994 cm^{-1} are characteristic of the vibrational stretching modes of W=O in the WO_4^{2-} unit. Furthermore, the intense bands in the range 751-773 cm^{-1} correspond to asymmetric stretching vibrations of W-O-W from the WO_4^{2-} unit.

Temperature programmed reduction studies were also useful in confirming the structure of the catalysts and revealed additional information that was not evident from XRD and Raman studies. For the TPR of the U/Mo catalyst the peak at 614 °C was due to the reduction of U^{6+} in the uranyl ion to U^{4+}, the equivalent U^{6+} to U^{4+}peak was in the reduction profile of UO_3 to UO_2 at 690 °C [19]. It appears that the reduction of uranium in the U/Mo catalyst is more facile than in the single oxide, due to modification of the U^{6+} ion. The reduction features at 653 and 780 °C were most likely due to reduction of Mo^{6+} to Mo^{4+} and Mo^{4+} to Mo^0 respectively. The reduction of molybdenum from Mo^{6+} in MoO_3 is generally observed at higher temperatures than those observed for the uranyl molybdate phase from this study [19,20]. It is therefore clear that the formation of the mixed oxide influences the redox behaviour of the uranium and molybdenum ions.

The formation of the Fe/Mo mixed oxide also facilitated the reduction process compared to the single component oxides. The mechanism of reduction for the Fe/Mo mixed oxide has been investigated in detail previously [21,22]. The four peaks in the TPR corresponded well with data in previous studies, and the absence of any peaks in the regions 320-350 °C and 515-590 °C indicated the absence of any single iron oxide species, such as FeO, Fe_2O_3 and Fe_3O_4. The lowest temperature peak in the TPR profile was due to the reduction of $Fe_2(MoO_4)_3$ (ferric molybdate), to $FeMoO_4$, (ferrous molybdate) and leads to the formation of MoO_3 [22]. The features at 767 and 831 °C corresponded to the reduction of Mo^{6+} to Mo^{4+} in the two different environments of MoO_3 and MoO_4^{2-} [22]. The combination of iron and molybdenum oxide in the mixed oxide phase retarded the reduction of Fe3+ whilst facilitating the reduction of Mo6+ when the redox behaviour was compared to the component oxides. These data reinforce the conclusions from XRD and Raman studies, indicating the formation of a pure molybdate phase. Characterisation of the Fe/U oxide catalyst by XRD and laser Raman spectroscopy concluded that uranium oxide (UO_3) was the only identifiable phase, with no obvious evidence for the

formation of a mixed oxide or iron oxide phase. TPR studies of iron oxide, Fe_2O_3, showed a major reduction feature at 586 °C, with a much smaller reduction feature at 350 °C, whilst Fe_3O_4 showed a major reduction feature at 655 °C for the oxide alone. Furthermore, studies of the reduction of UO_3 produced a broad reduction feature at 690 °C, in a similar temperature range expected for the iron oxides. It is difficult to unequivocally assign the reduction peaks of the Fe/U catalyst, however, the peak at 489 °C is assigned to the reduction of UO_3. The reduction temperature is significantly lower than bulk UO_3 and it is clear that the presence of iron modifies the redox properties of UO_3. Further evidence to support this assignment is provided by the relative areas of the reduction profiles, uranium oxide is in a large excess compared with the iron component and hence the reduction feature at 489 °C is attributed to the uranium component. We have assigned the reduction peak at 576 °C to the reduction of FeO_X, this is close in temperature to the expected reduction for Fe_2O_3 at 586 °C. The smaller and lower temperature reduction peak expected at *ca.* 350 °C for Fe_2O_3 is not clearly visible, although it may be expected that the large reduction feature at 489 °C may interfere. Close analysis of the leading edge of the feature at 489 °C indicates that a further reduction feature is present at *ca.* 375 °C and leads into the main reduction peak. The assignment to FeO_X is consistent with the suggestion from the laser Raman data. The definite assignment of these reduction features cannot be certain, and it is possible that the order may be reversed. The co-precipitation procedure used to prepare the Fe/U catalysts resulted in an iron oxide phase with a highly dispersed small crystallite size. This would explain why the iron oxide phase was amorphous to X-rays and the increased indeterminate scattering capacity of small crystallites may also affect the Raman spectroscopy. However, in the case of the uranium and iron components the mixture of FeO_X and UO_3 facilitates the reduction of the oxides, and this is prevalent for UO_3 in particular.

Catalyst activity and by-product formation

The U/Mo, Fe/Mo and U/W oxide catalysts showed selective toluene oxidation activity and exhibited appreciable yields of benzaldehyde. It is interesting to note that all the selective catalysts contained either a molybdate or tungstate phase. Evidence from XRD, laser Raman and TPR studies indicated that the U/Mo and Fe/Mo catalysts consisted solely of the $UO_2(MoO_4)_2$ and $Fe_2(MoO_4)_3$ phases. The U/W oxide catalyst was predominantly the UO_2WO_4 phase with some WO_3 identified by XRD. The best catalyst for selective toluene oxidation was Fe/Mo. In the case of the Fe/Mo catalyst the presence of Fe in the molybdate phase was clearly beneficial. The Fe^{3+} ion can be considered as a Lewis acid site and it can aid the adsorption of the aromatic ring onto the catalyst surface [23]. The subsequent abstraction of a hydrogen atom from the toluene molecule by a basic site, could either occur by O^{2-} present as Mo=O or Mo-O-Mo bridging species. It is interesting to note that a similar catalyst has also been used previously for the selective oxidation of toluene [22]. However, direct comparison of catalyst performance cannot be made because previous studies by Kuang *et al*. have tested catalysts under very different conditions. For instance, catalytic tests were performed in the absence of molecular oxygen and in a pulse microreactor. The best yield of benzaldehyde obtained was 23.2 μmol g^{-1} for a Fe/Mo atomic ratio of 1:1. The results in this study, and the results of Kuang *et al.*, demonstrate that iron molybdates have an efficacy for selective toluene oxidation to benzaldehyde.

Although these studies were primarily concerned with the selective oxidation of toluene to benzaldehyde, it is also important to consider the influence of reaction by-products. The Fe/Mo catalysts exhibited a decrease in conversion as the temperature was increased and this was indicative of deactivation by blocking of the catalyst surface. In the reactor studies it was concluded that when the reaction temperature was reduced quickly from a catalytically active temperature the catalyst bed became solidified. This was most likely due to heavier molecular

weight species remaining on the catalyst surface. GC-MS analysis of the material extracted from the solidified catalyst bed indicated that products due to coupling reactions were formed, and included phthalic anhydride and methyl diphenylmethane. These were in addition to the more common benzaldehyde, benzoyl peroxide and benzoic acid products, and formation of these types of products have been reported previously [3,4,21]. Due to the deposition of the solid reaction products throughout the catalyst bed and the reactor it was not possible to quantify them. However, it was evident that the quantities of the solid reaction products deposited were much lower for U/Mo and U/W catalysts compared to Fe/Mo. Catalyst deactivation was not observed with the more unselective U/Mo and U/W oxidation catalysts, however, the yields of benzaldehyde were lower, and were produced at higher temperatures, therefore, potential precursors for by-product formation were only present at low concentrations and the higher temperature could aid the desorption of poisoning species from the catalyst surface.

In order to study the stability of benzaldehyde under reaction conditions and to probe the reaction pathway during toluene oxidation, benzaldehyde oxidation was attempted using the range of catalysts under equivalent conditions. Substantial amounts of solid products were always formed during reaction, and products were identified by NMR spectroscopy. Only one product was identified and this was benzoyl peroxide. According to these results it is likely that during toluene oxidation the primary benzaldehyde formed was subsequently oxidised rapidly to form benzoyl peroxide. Further studies on the partial oxidation of benzaldehyde were attempted in order to study the mechanism of partial oxidation, but unfortunately reproducible results could not be obtained, despite many efforts. This was due to the production of large quantities of solid material, which continually blocked the reactor and deactivated the catalyst under our reaction conditions. Previously, the study of benzaldehyde oxidation has not been widely investigated and this may be due to similar reasons of experimental difficulty. However, Martin *et al*. [4] observed that when using a vanadyl pyrophosphate catalyst, benzaldehyde was

strongly adsorbed on the catalyst surface, leading to the formation of cyclic anhydrides and degradation products of the aromatic ring. Various studies have reported the formation of benzoic acid from toluene oxidation [24,25], and although we did not detect it as a gaseous product it was detected as a solid product in the reactor. According to the results discussed above, and the literature studies, a possible scheme for toluene oxidation and reaction products can be proposed (Scheme 1).

It was clear from the results that coupling and more easily condensable products to form solids, such as benzoyl peroxide were only formed during toluene oxidation when benzaldehyde was observed, indicating that they were either formed by secondary reactions of a benzaldehyde intermediate or from a common surface intermediate. It appears most likely that a benzoate species could be formed as a reaction intermediate. This intermediate could lead either to the formation of benzoic acid, or to the formation of benzoyl peroxide through the reaction of two benzoate groups. The latter reaction was predominant in our benzaldehyde oxidation studies, and it is reasonable to assume that a similar mechanism also operates for benzaldehyde formed by toluene oxidation.

The oxide catalysts U/Sb, Fe/U and U/V did not exhibit any toluene selective oxidation activity. The Fe/U and U/V catalysts were active at the lowest temperatures and showed high selectivity towards carbon dioxide. The higher activity and absence of selective oxidation products can be related to the structural phases of these catalysts. Powder X-ray diffraction studies of the U/Fe oxide catalysts identified only UO_3, whilst this phase was also established by laser Raman spectroscopy, which suggested the presence of iron oxide, and this was confirmed by TPR. It has been shown that uranium oxides are, in general, very active for deep oxidation of a wide range of organic compounds to CO_X [26]. Furthermore, the characterisation studies are consistent with a dispersed iron oxide phase and it is recognised that catalysts of this type are

also active for total oxidation reactions [27]. The combination of these components would account for the observation of toluene total oxidation.

Similarly characterisation studies also showed that the U/V oxide catalyst was comprised from a mixture of the single oxides U_3O_8 and V_2O_5. Investigation of toluene oxidation using the same conditions employed to test the mixed oxide catalysts demonstrated that U_3O_8 produced 88% conversion to CO_2 at 300°C. Previously the total oxidation activity of U_3O_8 has been well documented, and using a considerably greater GHSV (70,000 h^{-1}) toluene was readily oxidised to CO_X at temperatures above 350 °C [28]. It was ther efore evident that in a similar manner to the Fe/U catalyst the mix of U_3O_8 and V_2O_5 single oxides were not suitable for selective toluene oxidation. Again no solid reaction products similar to those detailed above were produced, and this indicated that toluene was oxidised directly to CO and CO_2.

Relationship between structure and activity

It is clear that in this study the catalysts can be grouped into two classes, those, which are selective for toluene oxidation, such as U/Mo, Fe/Mo and U/W, and those, which only gave combustion products, such as U/Sb. U/V and Fe/U. The reactivity of the range of catalysts has also been studied for selective oxidation of saturated and unsaturated C_3 hydrocarbons [29]. In these previous studies Fe/Mo and U/Mo mixed oxide catalysts showing iron and uranium molybdate phases were relatively inactive for propane and propene oxidation. Outstanding results for the selective oxidation of propane and propene to formaldehyde were obtained using Fe/U catalysts prepared with ratios of 0.5/3 and 1/3. At 450 °C selectivity towards formaldehyde of 44% was achieved at 42% propane conversion. The mixed U/Sb catalyst, with an USb_3O_{10} structure, was inactive for propane oxidation, but demonstrated the expected high selective oxidation activity to form acrolein from propene [9, 10, 11]. The results of propane/propene oxidation show the reverse trend to toluene oxidation, that is catalysts; that are selective for C_3

oxidation are unselective for toluene and vice versa. It can therefore be concluded that catalyst features required for selective oxidation of aromatic compounds are very different from those needed for selective oxidation of saturated and linear unsaturated hydrocarbons.

5. Conclusions

Selective gas phase toluene oxidation to benzaldehyde was achieved using Fe/Mo, U/Mo and U/W mixed oxide catalysts; Fe/Mo was the most active and selective. The activity of Fe/U, Sb/U and V/U oxide catalysts produced only deep oxidation to carbon oxides. A range of by-products was observed, these were other partial oxidation and coupling products. By-product formation was particularly apparent for catalysts with high benzaldehyde yields. Preliminary studies of benzaldehyde oxidation suggest that they were derived from benzaldehyde, particularly for the production of benzyl peroxide.

Catalysts have been characterised by X-ray diffraction, Laser Raman spectroscopy and temperature programmed reduction. Pure molybdate phases were identified for the F e/Mo and U/Mo catalysts, and there was no evidence for the formation of single oxide phases. Data suggests that the formation of the molybdate ion is important for the selective oxidation of toluene to benzaldehyde. In contrast, the U/Fe catalyst was a mixture of U_3O_8 and V_2O_5, whilst the Fe/U catalyst was comprised of highly dispersed iron oxide on UO_3. The presence of the single oxides was responsible for toluene total oxidation. The U/Sb catalyst did not exhibit selective toluene oxidation, but previous studies have demonstrated that the catalyst exhibits high activity for selective propene oxidation. Similar behaviour has been observed for the other catalysts in this study, and it is apparent that catalysts that were selective for toluene oxidation were not selective for propene oxidation and vice versa.

Acknowledgements

The authors would like to thank Darren Lee at BNFL (Springfields, UK) for his assistance with this work and BNFL for financial support.

References

[1] L. Kesavan, R. Tiruvalam, M.H. Ab Rahim, M.I. bin Saiman, D.I. Enache, R.L. Jenkins, N. Dimitratos, J.A. Lopez-Sanchez, S.H. Taylor, D.W. Knight, C.J. Kiely, G.J. Hutchings, Science, 331 (2011), pp 195-199.

[2] W. Partenheimer, Catal. Today, 23 (1995), pp 69-158.

[3] J. Zhu, S.L.T Anderson, J. Chem. Soc. Faraday Trans., **85** (1989), 3629-3644.

[4] M. Ai, Heterogeneous Catalysis and Fine Chemicals II*"*, Elsevier Science Publishers B.V., Amsterdam, (1991).

[5] H.K. Matralis, C.H. Papadopoulou, C. Kordulis, A.A. Elguezabal, V.C. Coberan, Appl. Catal. A, **126** (1995), pp 365-380.

[6] A. Martin, U. Bentrup, A. Brückner, C. Lück, Catal. Lett., **59** (1999), pp 61-65.

[7] S.H. Taylor, Heterogeneous catalysis by uranium oxides, Metal Oxide Catalysts: Volume 2, (Eds. S.D. Jackson, J.S.J. Hargreaves), Wiley VCH, (2008), Chapter 13, pp 539-560.

[8] C.J. Machiels, A.W. Sleight, Proceedings of the 4th International Conference on Chemistry and Uses of Molybdenum, Climax. Molybdenum Co. Ann Arbor, Mich., (1982), p 411.

[9] R.K. Grasselli, J.L. Callahan, J. Catal., 14 (1969), pp 93-103.

[10] R.K. Grasselli, D.D. Suresh, K. Knox, J. Catal., 18 (1970), pp 356-358.

[11] R.K. Grasselli, D.D. Suresh, J. Catal., 25 (1972), pp 273-291.

[12] S.E. Golunski, T.G. Nevell, D.J. Hucknall, J. Catal., 88 (1984), pp 448-456.
[13] T.E. Albrecht-Schmitt, R.E. Sykora, J.E. King, A.J. Illies, J. Solid State Chem., 177 (2004), pp 1717-1722.
[14] K. Otsuka, Y. Wang, I. Yamanaka, A. Morikawa, J. Chem. Soc. Faraday Trans., **89** (1993), pp 4225-4230.
[15] M. Sundberg, B.D. Marinde, J. Solid State Chem., **121** (1996), pp 167-173.
[16] D.S. Kim, K. Segawa, T. Soeya, I.E. Wachs, J. Catal., **136** (1992), pp 539-553.
[17] N-L. Palacios, S.H. Taylor, Appl. Spectros., **54** (2000), pp 1372-1378.
[18] K. Aykan, A.W. Sleight, J. Am. Ceram. Soc., 53 (1970), pp 427-431.
[19] M-L. Palacios, Selective Oxidation Catalysts Based on Uranium Oxides, PhD Thesis, Cardiff University, (2000).
[20] P. Arnoldy, C. de Jonge, J.A. Mouljin, J. Phys. Chem., 89 (1985), pp 4517-4526.
[21] S. Lars, T. Anderson, J. Catal., **98** (1986), pp 138-149.
[22] W. Kuang, Y. Fan, K. Chen, Y. Chen, J. Chem. Res., 0 (1997), 366-367.
[23] A. Borgna, J. Sepúlveda, S.I. Magni, C.R. Apesteguia, Appl. Catal. A, 276 (2004), pp 207-215.
[24] J. Miki, Y. Osada, T. Konoshi, Y. Tachibana, T. Shikada, Appl. Catal. A, **137** (1996), pp 93-104.
[25] A.J. van Hengstum, J. Pranger, S.M. van Hengstum-Nijhuis, J.G. van Ommen, P.J. Gellings, J. Catal., 101 (1986), pp 323-330.
[26] G.J. Hutchings, C.S. Heneghan, I.D. Hudson, S.H. Taylor, ACS Symposium Series 638, Heterogeneous Hydrocarbon Oxidation, (Ed. B.K. Warren, S.T. Oyama), ACS Books Washington D.C., (1996), pp 58-75.
[27] S. Betteridge, C.R.A. Catlow, D.H. Gay, R.W. Grimes, J.S.J. Hargreaves, G.J. Hutchings, R.W. Joyner, Q.A. Pankhurst, S.H. Taylor, Topics Catal., **1** (1995), pp 103-110,

[28] G.J. Hutchings, C.S. Heneghan, I.D. Hudson, S.H. Taylor, Catal. Today, 59 (2000), pp 249-259.

[29] S.H. Taylor, G.J. Hutchings, M-L. Palacios, D.F. Lee, Catal. Today, 81 (2003), pp 171-178.

Table 1. Summary of catalysts BET Surface areas and phases identified from powder X-ray diffraction studies.

Catalyst	**At. ratio**	$SA_{BET}/m^2\ g^{-1}$	**Phases identified**
U/Mo	1/2	0.7	$UO_2(MoO_4)_2$
Fe/Mo	2/3	0.9	$Fe_2(MoO_4)_3$
U/Sb	1/3	25	USb_3O_{10}
Fe/U	0.5/3 1/3	18 116	UO_3 UO_3
U/V	1/3	0.8	U_3O_8, V_2O_5
U/W	1/3	1.5	UO_2WO_4, WO_3

Table 2. Laser Raman spectroscopy summary and assignment of U/Mo oxide catalyst and comparison with molybdenum and uranium reference compounds.

U/Mo oxide	$(NH_4)_6Mo_7O_{24}.H_2O$[a]	MoO_3[a]	$UO_2(AcO)_2$[b]	UO_2	α-U_3O_8	γ-UO_3	Band assignment
			207 (S)				UO_2^{2+} bending
	250, 224 (M)	290 (M), 283 (M), 245 (W), 217 (W)					δ bending vibration Mo-O- Mo of the $Mo_7O_{24}^{6-}$octahedral molybdate
347 (W)					343 (M) 351 (M)		U-O-IU sigma bending vibration
368 (W), 319 (W)	369-312 (W)						δ bending vibration Mo=O of the $Mo_7O_{24}^{6-}$octahedral molybdate
				450 (S)	412 (S) 483 (S)		U-O stretching vibration
761 (VS)					740 (M)	767 (S)	O-U-O-U symmetric stretching vibration
					811 (S)	838 (M)	U-O stretching vibration
799 (M), 793 (M), 747 (VS)	912-861 (M)	665 (M)					ν asymmetric Mo-O-Mo stretching vibration
886 (S)			881 (VS)				UO_2^{2+} symmetric stretching
		817 (VS)					ν symmetric stretching vibration Mo-O-Mo
955 (M)	938 (VS)	994 (S)					ν symmetric stretching vibration Mo=O

All frequencies in cm^{-1}. (VS) very strong, (S) strong, (M) medium, (W) weak

[a] [18,19] used to assist band assignment.

[b] [11,14,15] used to assist band assignment.

Table 3. Laser Raman spectroscopy summary and assignment of Fe/Mo oxide catalyst and comparison with iron oxide reference compound.

Fe/Mo oxide	**Fe_2O_3**	Band assignment
	289 (S), 220 (W)	bending vibration Fe-O-Fe
372, 362, 349, 300, 258 (M)		δ bending vibration Mo=O of the MoO_4^{2-} tetrahedral molybdate
		δ bending vibration Mo-O- Mo of the $Mo_7O_{24}^{6-}$octahedral molybdate
	405 (M)	asymmetric stretching vibration Fe-O-Fe
	603 (W)	symmetric stretching vibration Fe-O-Fe
783 (VS)		ν asymmetric Mo-O-Mo stretching vibration
821 (M)		ν asymmetric stretching vibration Mo=O of the MoO_4^{2-} tetrahedral molybd
967 (M), 937 (W)		ν symmetric stretching vibration Mo=O of the MoO_4^{2-} tetrahedral molybdate
991 (W)		ν symmetric stretching vibration Mo=O (MoO_3 crystalline phase)

All frequencies in cm^{-1}. (VS)= very strong, (S)=strong, (M)=medium, (W)=weak.

Table 4. Laser Raman spectroscopy summary and assignment of U/Sb oxide catalyst and comparison with antimony oxide reference compounds.

U/Sb oxide	**Sb_2O_3**	**Sb_2O_4**	Band assignment
205 (M), 304 (W)	259 (VS), 194 (S), 124 (W)	266 (M), 203 (VS), 147 (W)	δ bending vibration Sb-O-Sb (U-O-U)
345 (W), 401 (M), 464 (W), 491 (S), 560 (W)			ν symmetric + asymmetric stretching vibration $U\text{-}O_{I,IV}$, $Sb_I\text{-}O_I$, $Sb_{II}O_{I,}$ O_{III}, O_{IV}
	455 (VS), 378 (S), 361 (W)	651 (M), 618 (VW), 467 (M), 421 (Sh), 405 (S)	ν asymmetric stretching vibration Sb-O-Sb
	718 (M)	828 (VW), 755 (VW), 720(VW)	ν symmetric stretching vibration Sb-O-Sb
776 (M), 824 (W), 905 (M)		603 (W)	ν symmetric + asymmetric stretching vibration $U\text{-}O_{III}$, $Sb_I\text{-}O_{II}$, $Sb_{II}O_{II}$

All frequencies in cm^{-1}. (VS)= very strong, (S)=strong, (M)=medium, (W)=weak.

Table 5. Laser Raman spectroscopy summary and assignment of Fe/U oxide catalyst.

Fe/U oxide	Band assignment
	asymmetric stretching vibration Fe-O-Fe
332 (M)	asymmetric stretching vibration Fe-O-Fe
477 (W)	U-O stretching vibration
762 (S)	U-O stretching vibration
821 (W)	U-O stretching vibration

All frequencies in cm^{-1}. (VS)= very strong, (S)=strong, (M)=medium, (W)=weak.

Table 6. Summary and assignment of U/V oxide catalyst Raman spectroscopy and comparison with vanadium oxide reference compounds.

U/V oxide	**V_2O_5**	Band assignment
286 (S), 305 (M)	286 (S), 306 (M)	δ bending vibration V-O-V
406(M), 483 (M), 528 (S)	406(M), 483 (M), 528 (S)	ν symmetric stretching vibration V=O
703 (S)	702 (S)	ν asymmetric stretching vibration V-O-V
997 (VS)	995 (VS)	ν symmetric stretching vibration V-O-V

All frequencies in cm^{-1}. (VS)= very strong, (S)=strong, (M)=medium, (W)=weak.

Table 7. Laser Raman spectroscopy summary and assignment of U/W oxide catalyst and comparison with tungsten oxide reference compound.

U/W oxide	**WO_3**	Band assignment
241 (W), 272 (M), 326 (W), 355 (W)	229 (W), 273 (M), 311 (W), 327 (W)	δ bending vibration W-O-W
	577 (W)	ν asymmetric stretching vibration W-O-W
717 (S)	717 (S)	ν asymmetric stretching vibration W-O-W
751 (S), 773 (S)		ν symmetric stretching vibration O-U-O-U
806(VS)	806 (VS)	ν symmetric stretching vibration W-O-W
883 (M)		UO_2^{2+} symmetric stretching
866 (W), 909 (W)		ν symmetric stretching vibration W-O-W of the WO_4^{2-}
953 (W)		ν asymmetric stretching vibration W=O of the WO_4^{2-}
994 (W)		ν symmetric stretching vibration W=O of the WO_4^{2-}

All frequencies in cm^{-1}. (VS)= very strong, (S)=strong, (M)=medium, (W)=weak.

Table 8. Toluene conversion and selectivity to benzaldehyde during the oxidation of toluene over different mixed oxide catalysts

Catalyst	Temperature / °C	Conversion /%	Benzaldehyde selectivity /%	CO selectivity /%	CO_2 selectivity /%
U/Mo	300	0	-	-	-
1:2	425	62	5	10	85
	450	88	8	14	78
	500	90	13	30	57
Fe/Mo[a]	300	0	-	-	-
2:3	400	43	86	0	14
	450	33	0	0	100
	500	13	0	0	100
U/Sb	300	0	-	-	-
1:3	450	12	0	0	100
	500	27	0	0	100
	530	28	0	0	100
Fe/U	200	0	-	-	0
0.5:3	300	69	0	4	96
	350	82	0	3	97
	450	89	0	3	97
U/V	200	0	-	-	-
1:3	300	30	0	0	100
	350	83	0	0	100
	400	100	0	0	100
U/W	300	0	-	-	-
1:3	400	13	0	0	100
	425	24	0	0	100
	450	41	0	0	100
	475	74	5	13	82
	500	87	8	14	78
Blank	200	0	-	-	-
reaction	300	0	-	-	-
	400	0	-	-	-
	500	Tr.	-	-	-

GHSV = 3700 h^{-1}, O_2/Toluene/He = 16/1/83, toluene = 6.8×10^{-4} mol h^{-1}.

[a] Catalyst deactivation observed at 450 and 500 °C

Captions for Figures and Scheme

Figure 1. Laser Raman spectrum of the U/Mo oxide catalyst.

Figure 2. Laser Raman spectrum of the Fe/Mo oxide catalyst.

Figure 3. Laser Raman spectrum of the U/Sb oxide catalyst.

Figure 4. Laser Raman spectrum of the Fe/U oxide catalyst.

Figure 5. Laser Raman spectrum of the U/V oxide catalyst.

Figure 6. Laser Raman spectrum of the U/W oxide catalyst.

Figure 7. Temperature programmed reduction profile of the U/Mo mixed oxide catalyst: 25 mg catalyst, 10 °C min^{-1}, 10% H_2/Ar.

Figure 8. Temperature programmed reduction profile of the Fe/Mo mixed oxide catalyst: 25 mg catalyst, 10 °C min^{-1}, 10% H_2/Ar.

Figure 9. Temperature programmed reduction profile of the U/W mixed oxide catalyst: 100 mg catalyst, 10 °C min^{-1}. 10% H_2/Ar.

Figure 10. Temperature programmed reduction profile of the Fe/U mixed oxide catalyst: 70 mg catalyst, 10 °C min^{-1}, 10% H_2/Ar.

Scheme 1. Possible scheme for the formation of benzoyl peroxide during the oxidation of toluene.

Figure 1.

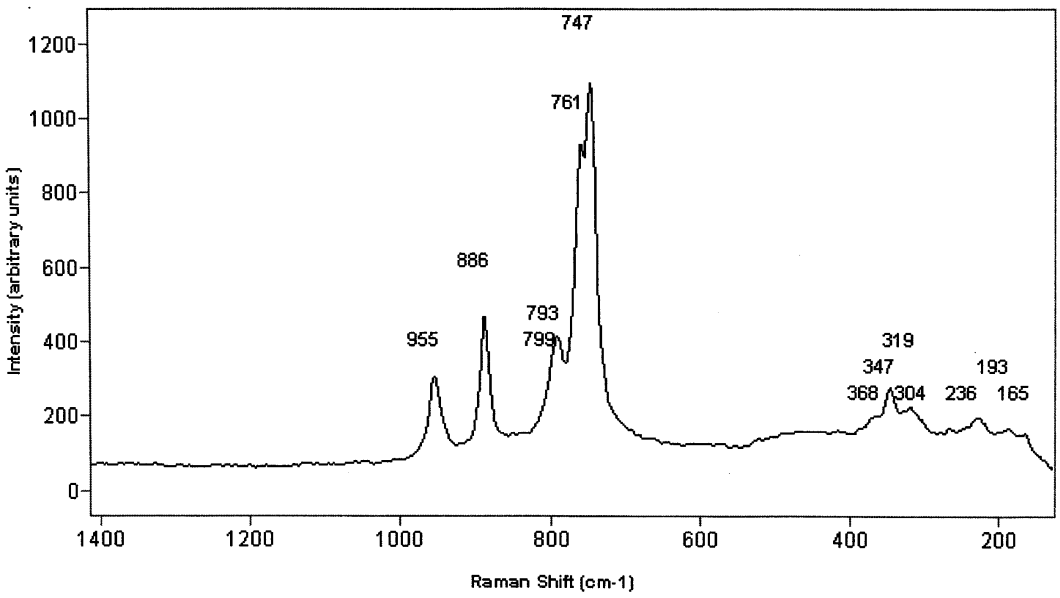
747
761
886
793
799
955
319
347
368
304
236
193
165
1200
1000
800
600
400
200
0
1400
1200
1000
800
600
400
200
Intensity (arbitrary units)
Raman Shift (cm-1)

Figure 2.

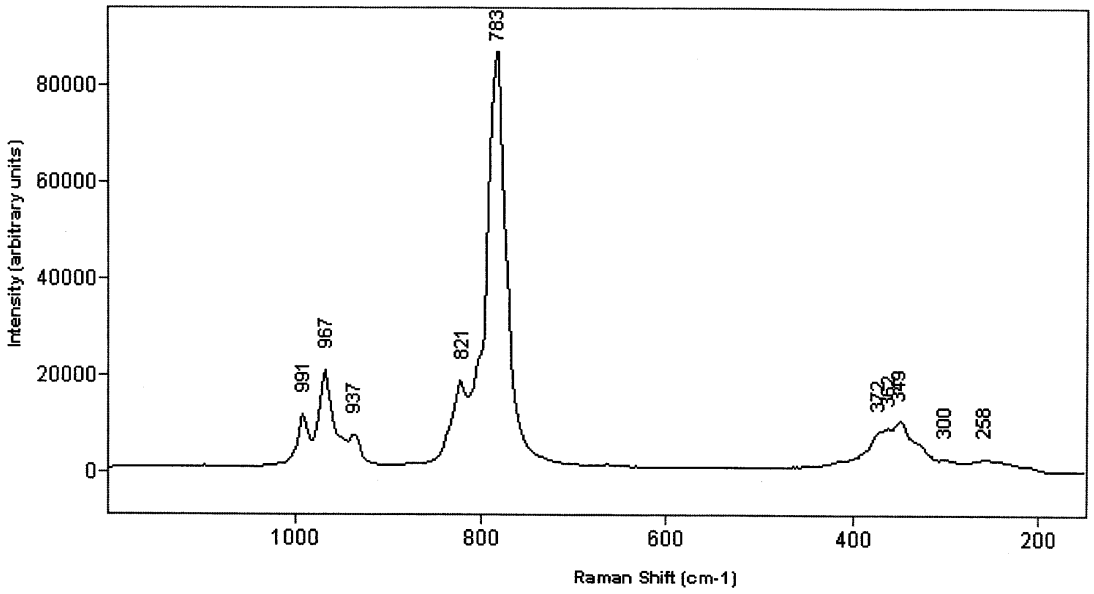
Intensity (arbitrary units)
80000
60000
40000
20000
0
991
967
937
821
783
372
356
349
300
258
1000
800
600
400
200
Raman Shift (cm-1)

Figure 3.

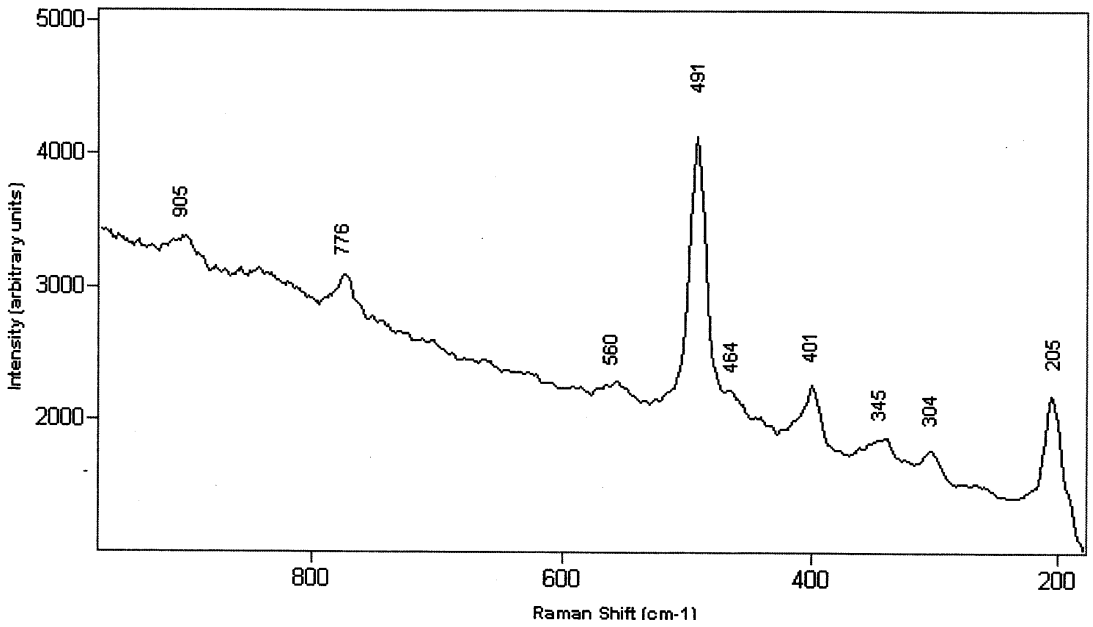
5000
4000
3000
2000
Intensity (arbitrary units)
905
776
560
491
464
401
345
304
205
800
600
400
200
Raman Shift (cm-1)

Figure 4.

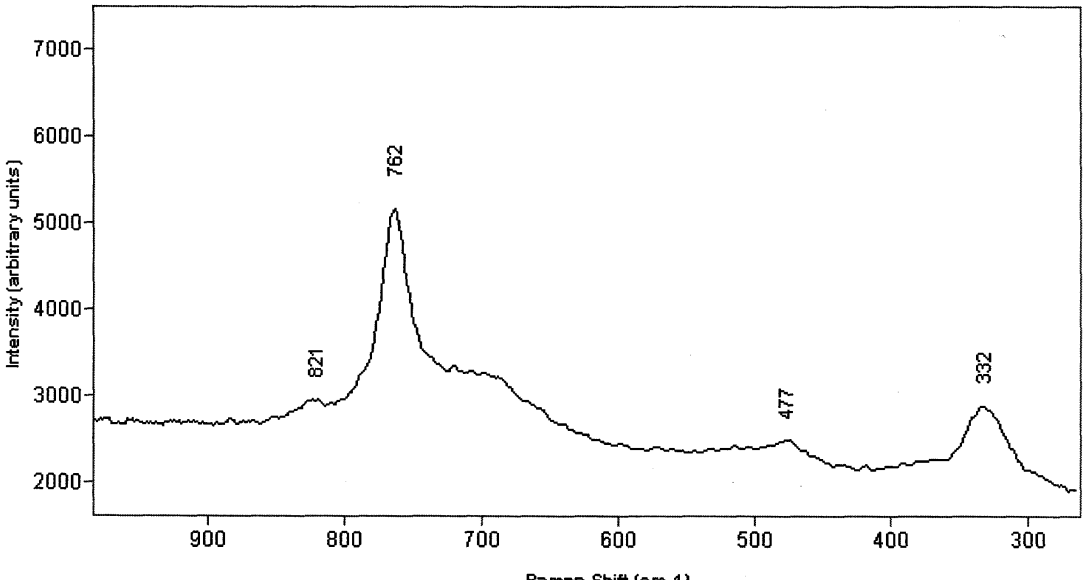
Intensity (arbitrary units)
7000
6000
5000
4000
3000
2000
900
800
700
600
500
400
300
821
762
477
332

Figure 5.

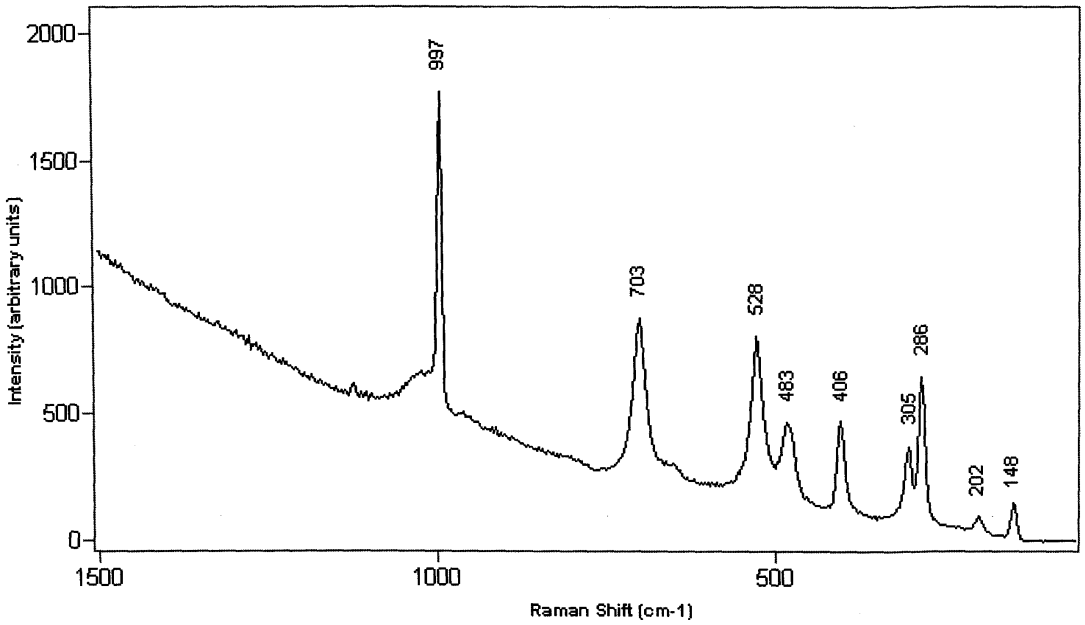
2000
1500
1000
500
0
Intensity (arbitrary units)
997
703
528
483
406
305
286
202
148
1500
1000
500
Raman Shift (cm-1)

Figure 6.

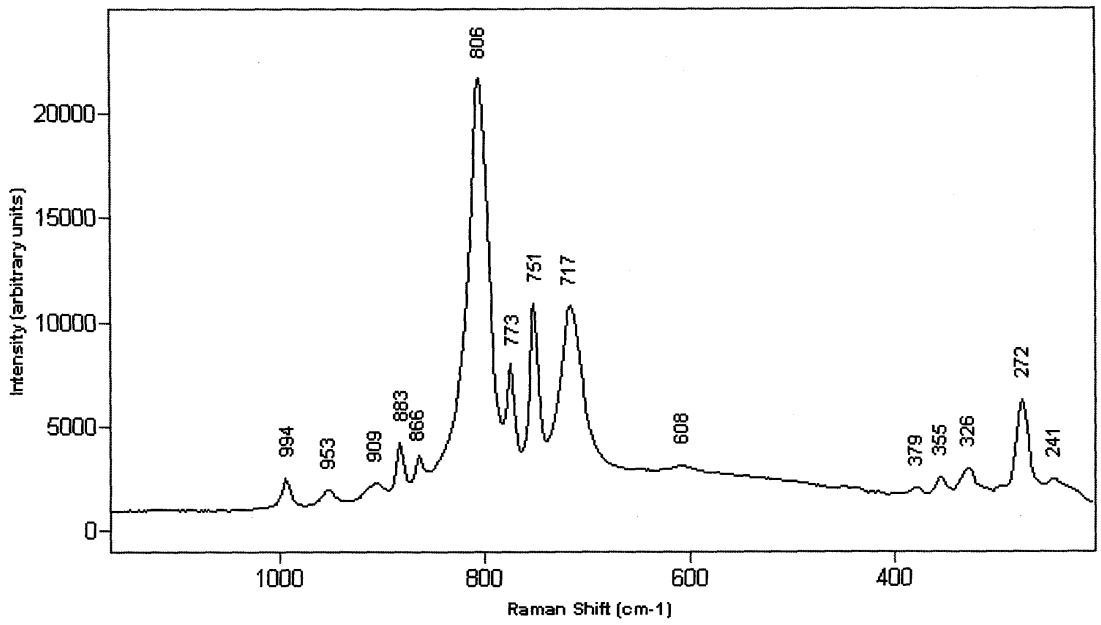
Intensity (arbitrary units)
20000
15000
10000
5000
0
1000
800
600
400
Raman Shift (cm-1)
994
953
909
883
866
806
773
751
717
608
379
355
326
272
241

Figure 7.

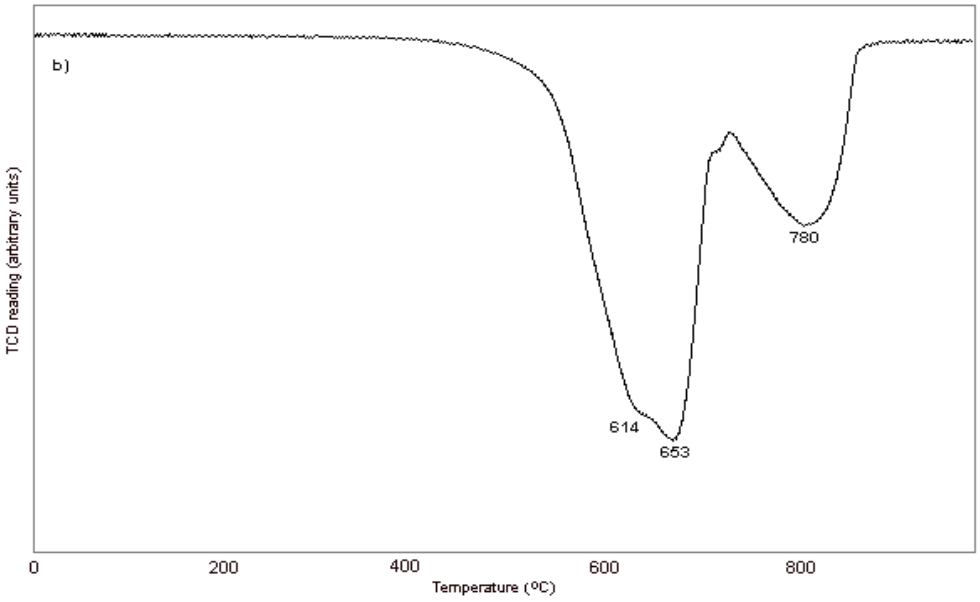
b)
TCD reading (arbitrary units)
614
653
780
0
200
400
600
800
Temperature (°C)

Figure 8.

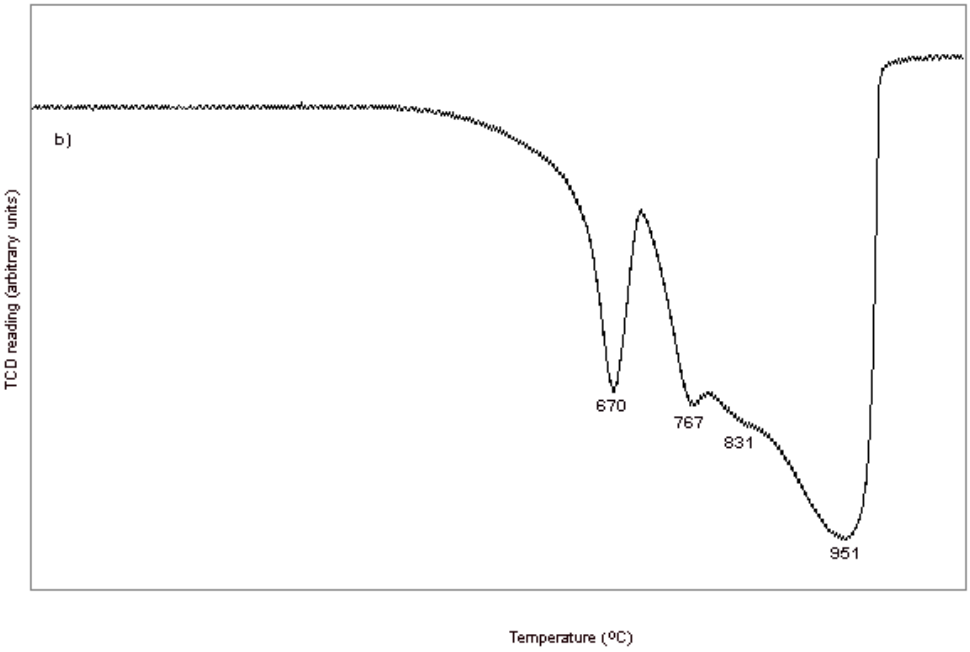
b)
TCD reading (arbitrary units)
670
767
831
951
Temperature (ºC)

Figure 9.

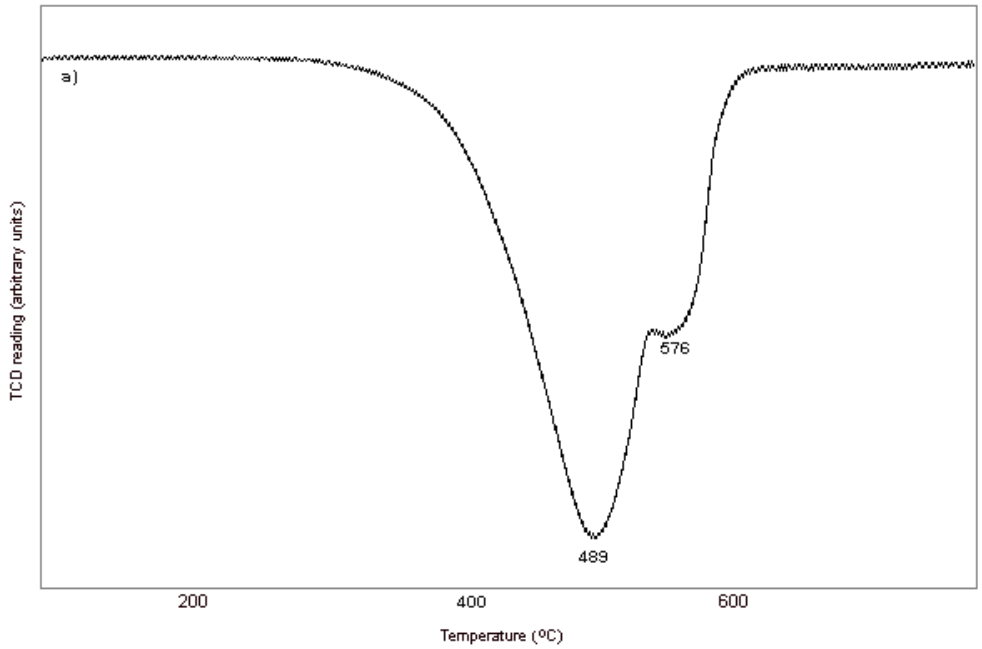
a)
576
489
TCD reading (arbitrary units)
200
400
600
Temperature (°C)

Figure 10.

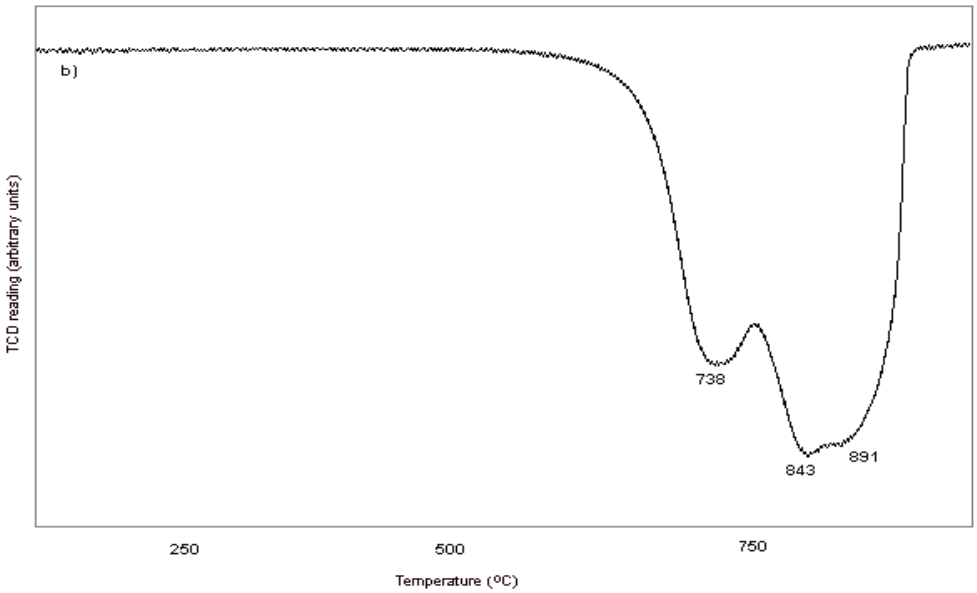
b)
TCD reading (arbitrary units)
738
843
891
250
500
750
Temperature (°C)

Scheme **1.**

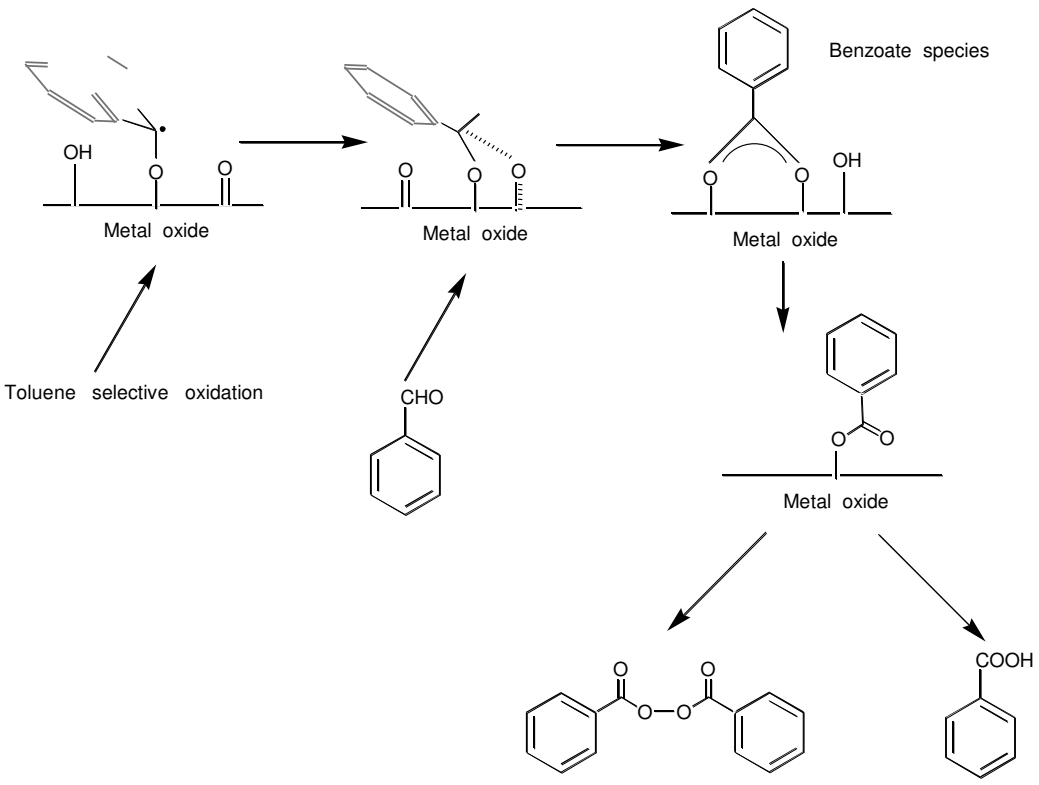
Benzoate species
OH
O
O
Metal oxide
O
O
O
Metal oxide
O
O
OH
Metal oxide
Toluene selective oxidation
CHO
O
O
Metal oxide
O
O
O
O
COOH